Supplemental material to this article can be found at:
http://molpharm.aspetjournals.org/content/suppl/2023/07/07/molpharm.122.000658.DC1
1521-0111/104/4/133–143$35.00
MOLECULAR PHARMACOLOGY
dx.doi.org/10.1124/molpharm.122.000658
Mol Pharmacol 104:133–143, October 2023
Copyright © 2023 by The American Society for Pharmacology and Experimental Therapeutics

Licochalcone Mediates the Pain Relief by Targeting the Voltage-Gated Sodium Channel[S]

Qianru Zhao,[1] Xu Zhang,[1] Siru Long,[1] Shaobing Wang, Hui Yu, Yongsheng Zhou, Yi Li, Lu Xue, Yan Hu, and Shijin Yin

Department of Chemical Biology, School of Pharmaceutical Sciences, South-Central Minzu University, Wuhan, People's Republic of China (Q.Z., X.Z., S.L., S.W., H.Y., Y.Z., Y.H., S.Y.) and Institute for Medical Biology and Hubei Provincial Key Laboratory for Protection and Application of Special Plants in Wuling Area of China, College of Life Sciences, South-Central Minzu University, Wuhan, People's Republic of China (Y.L., L.X.)

Received November 27, 2022; accepted June 8, 2023

ABSTRACT

Licorice is a traditional Chinese medicine and recorded to have pain relief effects in national pharmacopoeia, but the mechanisms behind these effects have not been fully explored. Among the hundreds of compounds in licorice, licochalcone A (LCA) and licochalcone B (LCB) are two important components belonging to the chalcone family. In this study, we compared the analgesic effects of these two licochalcones and the molecular mechanisms. LCA and LCB were applied in cultured dorsal root ganglion (DRG) neurons, and the voltage-gated sodium (Na_V) currents and action potentials were recorded. The electrophysiological experiments showed that LCA can inhibit Na_V currents and dampen excitabilities of DRG neurons, whereas LCB did not show inhibition effect on Na_V currents. Because the $Na_V1.7$ channel can modulate Subthreshold membrane potential oscillations in DRG neuron, which can palliate neuropathic pain, HEK293T cells were transfected with $Na_V1.7$ channel and recorded with whole-cell patch clamp. LCA can also inhibit $Na_V1.7$ channels exogenously expressed in HEK293T cells. We further explored the analgesic effects of LCA and LCB on formalin-induced pain animal models. The animal behavior tests revealed that LCA can inhibit the pain responses during phase 1 and phase 2 of formalin test, and LCB can inhibit the pain responses during phase 2. The differences of the effects on Na_V currents between LCA and LCB provide us with the basis for developing Na_V channel inhibitors, and the novel findings of analgesic effects indicate that licochalcones can be developed into effective analgesic medicines.

SIGNIFICANCE STATEMENT

This study found that licochalcone A (LCA) can inhibit voltage-gated sodium (Na_V) currents, dampen excitabilities of dorsal root ganglion neurons, and inhibit the $Na_V1.7$ channels exogenously expressed in HEK293T cells. Animal behavior tests showed that LCA can inhibit the pain responses during phase 1 and phase 2 of formalin test, whereas licochalcone B can inhibit the pain responses during phase 2. These findings indicate that licochalcones could be the leading compounds for developing Na_V channel inhibitors and effective analgesic medicines.

Introduction

Licorice is a commonly used traditional Chinese medicine consisting of *Glycyrrhiza uralensis* Fisch., *Glycyrrhiza inflata* Batalin, and *Glycyrrhiza glabra* L. according to Chinese national pharmacopoeia (The Committee of Pharmacopoeia of the People's Republic of China, 1995). The efficacy of licorice decoction includes stomach and spleen protection, pain relief, cough alleviation, and phlegm elimination recoded in ancient Chinse medicine archives (Yang et al., 2015). More beneficial effects of licorice on multiple diseases were found with broader investigations in recent years. It is reported that licorice or its extracts have antiviral and antimicrobial activities (Ahn et al., 2012; Adianti et al., 2014). Recent studies also indicate that licochalcone A (LCA) could relieve the neuropathic pain in chronic constriction injury model and the inflammatory responses induced by lipopolysaccharide (Chu et al., 2012; Li et al., 2021).

The general effects of licorice could be explained by its complex constituents. For now, at least 20 triterpenoids and 300 flavonoids were found in licorice, and each component has specific activities (Yang et al., 2015). This may explain why

This work is supported partly by grants from the National Natural Sciences Foundation of China [81373379 and 81641186] and the National Key R and D Program of China [2019YFC1712402] (to S.Y.); the National Natural Sciences Foundation of China [32000685] and Natural Sciences Foundation of Hubei Province [2020CFB348] (to Q.Z.); the Fundamental Research Funds for the Central Universities, South-Central Minzu University [CZZ19005] (to S.Y.) and [CZQ23026] (to Q.Z.); and Knowledge Innovation Program of Wuhan-Shuguang Project [2022020801020412] (to Q.Z.).
All authors declare no interest conflicts.
[1]Q.Z., X.Z., and S.L. contributed equally to this work.
dx.doi.org/10.1124/molpharm.122.000658.
[S] This article has supplemental material available at molpharm.aspetjournals.org.

ABBREVIATIONS: APP, action potential peak; DMEM, Dulbecco's modified eagle medium; DRG, dorsal root ganglion; Ep, Eppendorf; gNa, membrane conductance of Na^+; HBSS, Hank's balanced salt solution; HPLC, high performance liquid chromatography; I, amplitude of peak current; I-V curve, current-voltage curve; I_{Na}, sodium current; $I_{vehicle}$, amplitude of Na_V current after the vehicle treatment; LCA, Licochalcone A; LCB, Licochalcone B; LrB, loureirin B; Na_V, voltage-gated sodium; Opti-MEM, opti-minimal essential medium; RP, resting membrane potential; TTX, tetrodotoxin.

the effects of licorice are various, but the mechanisms of these effects are little known. With the development of extraction and identification techniques, single molecules in licorice have been isolated, synthesized, and tested under physiologic situations. The molecular mechanisms behind the effects could be unveiled gradually. Among the hundreds of compounds in licorice, LCA is the one that attracted the most attention. The main reports about LCA are related to its antitumor effects (Yang et al., 2015; Hong et al., 2019). We compared the backbone of LCA and another kind of chalcone, loureirin B (LrB), and found that they have high similarities with each other. Since LrB was reported to be a voltage-gated sodium (Na_V) channel blocker and have analgesic effects (Chen et al., 2018), we applied LCA in cultured dorsal root ganglion (DRG) neurons and found that it could inhibit Na_V currents and dampen excitabilities of DRG neurons. Then we compared the effects of licochalcone B (LCB), which is also a component of licorice and shares the same basic structure with LCA (Yang et al., 2015). We found that LCB did not significantly inhibit the Na_V currents in DRG neurons. These differences of the effects on Na_V currents between LCA and LCB may provide us with the basis for developing specific Na_V channel inhibitors.

Na_V channels are reported to consist of 10 different pore-forming α subunits ($Na_V1.1$–9 and Na_VX) (Dib-Hajj and Waxman, 2019). Among them, $Na_V1.7$ is mainly expressed in the nociceptors and peripheral neurons, such as DRG neurons, thus $Na_v1.7$ channel has become a potential drug target for pain (Ho and O'Leary, 2011; Li et al., 2018). $Na_V1.7$ channel could modulate subthreshold membrane potential oscillations in DRG neurons, which can palliate neuropathic pain (Li et al., 2018; McDermott et al., 2019). Gain-of-function mutation in $Na_V1.7$ expressing gene SCN9A was related to inherited erythromelalgia (Yang et al., 2004; Fertleman et al., 2006), whereas loss-of-function mutation in SCN9A was linked to channelopathy-associated congenital insensitivity (indifference) to pain and hereditary sensory and autonomic neuropathy type IID (Gingras et al., 2014; Yuan et al., 2013). Inhibition of $Na_V1.7$ might alleviate pain with few side effects because of its exclusive expression in nociceptors, but the number of effective and specific $Na_V1.7$ inhibitors is still rare (Kingwell, 2019). In this research, we found that LCA could block the Na_V currents in DRG neurons and the $Na_V1.7$ channels exogenously expressed in HEK293T cells. Further investigations in animal behavior tests showed that LCA could inhibit the pain responses during phase 1 and phase 2 of the formalin test. These are novel findings that revealed the analgesic effects of licochalcones and the molecular mechanisms related to inhibition on voltage-gated sodium channel. This study indicates that licochalcones have the potential to be developed into effective analgesic medicines.

Materials and Methods

Chemicals. Poly-D-lysine (Cat. E607014) and Hanks' balanced salt solution (HBSS) (Cat. A003210) were ordered from Sangon Co., Ltd (Shanghai, China). Opti-minimal essential medium (Opti-MEM) (Cat. 31985070), Dulbecco's modified eagle medium (DMEM) (Cat. 11965092), Neurobasal-A (Cat. 10888022), and B-27 supplement (Cat. 17504044) solutions were bought from Gibco (New York, NY), and FBS was ordered from YEASON (Suzhou, China). LCA (Cat. B20409) and ATP-Mg (Cat. T31046) were bought from Yuanye Bio-Technology Co., Ltd (Shanghai, China). The purities of LCA and LCB were high performance liquid chromatography (HPLC) ≥98.0%, and the accuracy of LCA and LCB structures were confirmed by nuclear magnetic resonance technology. LCA and LCB were dissolved in DMSO and diluted with the external solution for electrophysiological experiment, and the same volume of DMSO was added as the vehicle group. Penicillin-streptomycin (Cat. C0230) was bought from Nobleryder (Peking, China), papain (Cat. BS-190) from Biosharp (Hefei, China), and collagenase (Cat. 11179179001) and dispase (Cat. 04942078001) from Roche (Basel, Switzerland). Borosilicate glass (Cat. B15013F) was bought from VitalSense Scientific Instruments Co., Ltd (Wuhan, China) and ExFect2000 Transfection Reagent (Cat. T202-01) from Vazyme (Nanjing, China). Mexiletine (Cat. 5370-01-4) was bought from Aladdin (Shanghai, China) and DMSO (Cat. D2650) from Sigma-Aldrich (St. Louis, MO). Chloral hydrate (Cat. 30037516) and 37% formalin solution (Cat. 33314) were ordered from Sinopharm Chemical Reagent Co., Ltd (Shanghai, China).

Plant Materials. The names of the licorice used in our research have been checked on http://www.theplantlist.org. *G. inflata* Batalin was bought from Yarkand County Fuyuan Licorice Co., Ltd. (Yarkand, Xinjiang, China). Its flavonoids were extracted according to the methods previously reported (Miyazaki et al., 2020). Roots of *G. inflata* Batalin were ground into powder, and ethyl acetate was added. The mixture was refluxed at 75°C for 2 hours, and the drug residues were removed. The solvent was dried with nitrogen, and methanol was added for HPLC analysis. Agilent 1100 liquid chromatograph with Agilent SDB C18 chromatographic column (Santa Clara, CA) was used for HPLC analysis. Mobile phase A is 0.5% phosphoric acid aqueous solution, and mobile phase B is acetonitrile. The gradient elution program is as follows: 0→5 minutes, B from 30%→40%; 5→7 minutes, B rose to 50%; 7→30 minutes, B rose to 55%. The detection wavelength was 372 nm, and the flow rate was 1.0 mL/min. The quantities of the licochalcones were measured according to the peak area of the HPLC chromatography. The content of LCA is 2.22% in *G. inflata* Batalin and 22.20% in its extract. The *G. inflata* Batalin extract was applied with 0.046 mg/mL mass:volume ratio in electrophysiological experiment to guarantee that the molar concentration of LCA was 30 μM. *G. uralensis* Fisch. flavonoids were bought from FEIYUBIO Co., Ltd (Cat. FY1246, Nantong, Jiangsu, China). The same mass:volume ratio of *G. uralensis* Fisch. flavonoids were applied as negative control because it does not contain LCA or LCB according to HPLC analysis. The *G. inflata* Batalin extract and *G. uralensis* Fisch. flavonoids were dissolved in DMSO and diluted with the external solution for electrophysiological experiment. The same volume of DMSO was added as the vehicle group. The inhibition rate of Na_V current in DRG neuron was calculated as follows:

$$\text{Inhibition rate} = (I_{vehicle} - I_{drug})/I_{vehicle} \quad (1)$$

Where I_{drug} represents the amplitude of Na_V current after the drug treatment, and $I_{vehicle}$ represents the amplitude of Na_V current after the vehicle treatment.

Preparation of Dorsal Root Ganglion Neurons. Experiment animals were bought from Wuhan Center for Disease Control and Prevention. All animal experiments were conducted according to the rules of the National Institutes of Health Guide for the Care and Use of Laboratory Animals and strictly following guidelines of the Institutional Animal Care and Use Committees. The Institutional Animal Care and Use Committees checked all protocols, and the animal ethical approval number is 2020-scuec-028. Four-week-old female Kunming mice were anesthetized with isoflurane and sacrificed. The whole spine was dissected out and put in ice-cold HBSS. Extra muscles and tissues were discarded. The spine was cut along the middle line into two symmetrical parts with scissors. Dorsal root ganglions were picked under dissecting microscope. Fibers on DRG were trimmed, and only transparent ganglions were left. The round ganglions were lysised with 2 mg/mL papain in HBSS for 10 minutes at 37°C. During this time, the Eppendorf (Ep) tubes containing ganglions were shaken frequently. The Ep tubes were centrifuged at 4200 rpm for 4 minutes. The supernatant was discarded, and the precipitates were resuspended with

3.75 mg/mL collagenase and 3.75 mg/mL dispase for 10 minutes at 37°C. The Ep tubes were centrifuged at 4200 rpm for 4 minute again. The supernatant was discarded, and 1 mL DMEM was added to stop enzyme digestions. DRG neurons were dissociated by trituration with a fire-polished glass Pasteur pipette (Liu et al., 2009). The cells were centrifuged and resuspended, and seeded on coverslips preincubated with 10 μg/mL poly-D-lysine. Cells were cultured for 2 hours, and extra culture medium (Neurobasal-A with 1× B-27 supplement) was added. After more than 16 hours, DRG neurons were used for electrophysiology recordings.

HEK293T Cell Culture and Transfection. HEK293T cell is a gift from Jing Yao laboratory (School of Life Sciences, Wuhan University, China). The cells were seeded in 24-well plate and cultured in DMEM with 10% FBS and 1% penicillin-streptomycin. When the cell density reached 60%–80%, the cells were transfected with plasmids expressing the human $Na_V1.7$ channel. The transfection procedure was briefly introduced as follows: 800 ng pcDNA3.1-SCN9A (NM_002977.3) plasmid, which expresses $Na_V1.7$, was cotransfected with pIRES2-EGFP plasmid expressing EGFP. Both pcDNA3.1 and pIRES2-EGFP plasmids are gifts from Wenxin Li laboratory (School of Life Sciences, Wuhan University, China). The full-length cDNAs for human $Na_V1.7$ (SCN9A) were subcloned into pcDNA3.1 and sequenced. The HEK293T cells were transfected as the process reported previously (Shi et al., 2021). One Ep tube contained 40 μL Opti-MEM mixed with pcDNA3.1-SCN9A and pIRES2-EGFP plasmids; another one contained 2 μL ExFect2000 in 40 μL Opti-MEM. The two solutions were kept still for 5 minutes without disturbance. After that, they were mixed and left for 20 minutes again. The mixed solution was added gently in the culture medium of HEK293T cells and incubated for more than 36 hours. When the expression of $Na_V1.7$ and EGFP was confirmed with fluorescence microscope, cells were resuspended and seeded on coverslips. After the cells attached on the coverslips, they were picked for electrophysiology recordings.

Electrophysiological Study. Whole-cell patch-clamp recordings were performed using an EPC9 amplifier (HEKA Elektronik, Lambre-cht/Pfalz, Germany) at room temperature (22–24°C). Pipettes pulled from borosilicate glass had resistances of 2–4 MΩ when filled with the internal solution. The internal pipette solution for recording Na_V currents contained 130 mM CsCl, 9 mM NaCl, 1 mM $MgCl_2$, 10 mM EGTA, and 10 mM HEPES (pH 7.3 with CsOH) (Chang et al., 2018). The external solution for recording Na_V currents contained 131 mM NaCl, 10 mM TEACl, 10 mM CsCl, 3 mM 4-aminopyridine, 2 mM $MgCl_2$, 1 mM $CaCl_2$, 0.3 mM $CdCl_2$, 10 mM HEPES, and 10 mM glucose (pH 7.4 with NaOH) (Chang et al., 2018). Electrophysiology data were analyzed using IGOR (WaveMetrics; Lake Oswego, OR) software. Series resistance was compensated by 80%.

The holding potential was set at −120 mV. Sodium currents (I_{Na}) were elicited from −80 mV to +15 mV in 5-mV steps for 50 milliseconds (Zheng et al., 2018). The interval between sweeps lasted for 5 seconds. We evaluated steady-state I_{Na} activation by measuring membrane conductance of Na^+ (g_{Na}), which was determined with the equation

$$g_{Na} = I_{Na}/(V_m - V_{rev}) \quad (2)$$

where V_m is the membrane potential, and V_{rev} is the observed reversal potential for Na^+ calculated through current-voltage (I-V) curve. $g_{Na}/g_{Na\text{-}max}$ was plotted against membrane potential, and the putative curve was fitted with a sigmoidal function using the Boltzmann model:

$$g_{Na}/g_{Na-max} = 1/\{1+\exp[(V_{m1/2} - V_m)/k]\} \quad (3)$$

The half-activation voltage was gotten from the fitness curve. For fast inactivation curves, currents were elicited from −130 mV to 0 mV in 10-mV steps for 500 milliseconds, then kept at 0 mV for 20 milliseconds. For slow inactivation curves, currents were elicited from −140 mV to 20 mV in 10-mV steps for 10 seconds, then hyperpolarized to −120mV for 20 milliseconds and depolarized to 0 mV for 20 milliseconds. The currents elicited by depolarization after preconditional voltage steps were analyzed (Goldfarb et al., 2007; Zheng et al., 2018). The half-inactivation voltage was gotten by fitting $I_{Na}/I_{Na\text{-}max}$ against membrane potential with a sigmoidal function using Boltzmann model:

$$I_{Na}/I_{Na-max} = 1/1+\exp[(V_{m1/2} - V_m)/k]\} \quad (4)$$

For the current clamp recording on DRG neurons, the internal pipette solution contained 140 mM KCl, 0.5 mM EGTA, 5 mM HEPES, and 3 mM Mg-ATP (pH 7.3 with KOH). The external solution for current clamp recording contained 140 mM NaCl, 3 mM KCl, 2 mM $MgCl_2$, 2 mM $CaCl_2$, and 10 mM HEPES (pH 7.3 with NaOH). Cells with rest membrane potential greater than −50 mV were discarded. Cells were clamped at the resting membrane potential (RP) and elicited with 0–1000 pA ramp current for 500 milliseconds. After the cell state is stable, the action potentials of DRG neurons were recorded before and after drug administration. The number of action potentials, RP, neuronal action potential peak (APP), and action potential threshold were compared before and after the drug treatments. APP was determined by the difference between the APP and the minimum voltage after hyperpolarization, and action threshold was determined by the membrane potential that generated the action potential (Dustrude et al., 2016).

Tetrodotoxin (TTX)-sensitive Na_V currents were recorded in large-diameter (>30 μM) DRG neurons. After LCA treatment, the Na_V current was washed back to the level before LCA treatment with the external solution perfusion. 300 nM TTX diluted in external solution was applied and see whether TTX could inhibit the Na_v currents. The Na_V current, which could be completely inhibited by 300 nM TTX, was putative TTX-sensitive Na_V current, and the effects of LCA on TTX-resistant Na_V currents were tested in small-diameter (<30 μM) DRG neurons. We applied 300 nM TTX in the recording bath and perfusion solution to block the TTX-sensitive Na_V currents. The residual Na_V currents were putative TTX-resistant Na_V currents.

Animal Behavior Test. Animals used for the behavior test were 4-week-old female Kunming mice (20 g ± 2 g), which were commonly used mice strains for formalin-induced pain models (Zhong et al., 2012; Xu et al., 2019). Five to six mice per cage were housed and habituated to the environment for more than 1 week before the experiment. Behavior test was conducted during the daytime, starting at 9 AM in the morning. Mice were put in the observing box and habituated for 20 minutes. LCA or LCB were first diluted in DMSO (25 mg powder in 100 μL DMSO), then diluted in saline to make the final concentration. Mice were injected subcutaneously with different doses of LCA or licochalcone C, including 25 mg/kg, 50 mg/kg, and 100 mg/kg, 30 minutes before the formalin injection. The same volume of saline with diluted DMSO was injected subcutaneously as the vehicle group. The Nav channel blocker (IC_{50} for Nav1.7 is 1.77 mM) and analgesic drug mexilene were injected with a 50-mg/kg dose in the mice as positive control (Blackburn-Munro et al., 2002; Wu et al., 2013). Thirty minutes later, licochalcone, mexilene, and vehicle groups were injected with a 10-μL 2% formalin solution in the plantar of the right hind paws of the mice. Ten microliters of saline was injected in the plantar of the right hind paw as the saline group to screen out the effects of paw injection. Videos were recorded immediately after the paw injection for more than 30 minutes. The processes were separated into two phases. The first phase is 0–10 minutes, and the second phase is 15–30 minutes (McNamara et al., 2007). The time of mice licking their right hind paws was counted with a stopwatch by two-blinded analyzers.

Statistics Analysis. GraphPad Prism (San Diego, CA) was used to analyze the data. All data were tested for the normality first. Statistical analysis of differences was carried out using Student's *t* test or ANOVA combined with Turkey post hoc test if the data were normally distributed. Nonparametric statistical analysis was applied if the data did not distribute normally. $P < 0.05$ was considered significantly different. Using IGOR (WaveMetrics; Lake Oswego, OR) software, concentration-response curves of LCA were fitted according to the following modified Hill equation:

$$I_{LCA}/I_{vehicle} = 1/1+([LCA]/IC_{50}), \quad (5)$$

where I represents the amplitude of peak current, and [LCA] represent the concentration of LCA. The IC_{50} was gotten by four-parametric nonlinear regression analysis constraining bottom to 0 and top to 1.

Results

LCA Inhibits Na_V Current in DRG Neuron. LCA is a kind of chalcone extracted from licorice and shares similar backbone of chalcone structure with LrB (Fig. 1), which has been reported to significantly inhibit Na_V current in DRG neuron and has analgesic effects (Chen et al., 2018). We applied LCA to small-diameter (<30 μM) DRG neurons and recorded the Na_V currents to see whether LCA had similar effects with LrB on Na_V current. Our results showed that 30 μM LCA could significantly inhibit Na_V currents in DRG neurons (Fig. 2A). LCB is also a compound in licorice and shares similar backbone structures with LCA and LrB (Fig. 1). We tested the effects of LCB on small-diameter DRG neurons and recorded Na_V currents with patch-clamp technology. The voltage clamp results showed that LCB did not inhibit Na_V currents in DRG neurons (Fig. 2A).

We further recorded and analyzed gating properties of Na_V channel under LCA treatment. The maximum activation voltage was significantly higher in the 30-μM LCA treatment group (−12.73 ± 4.28 mV) than in the control (−15.45 ± 4.13 mV) and wash (−13.64 ± 4.72 mV) groups according to I-V curve (Fig. 2, B and C; Supplemental Fig. 1A). The activation and inactivation curves were fitted by single Boltzmann distributions (Griffith et al., 2019). The half-activation voltage was significantly higher in the 30-μM LCA treatment group (−18.21 ± 2.49 mV) than in the control (−25.41 ± 3.18 mV) and wash (−23.30 ± 1.01 mV) groups (Fig. 2D; Supplemental Fig. 1A), and half-inactivation voltage was significantly lower in the LCA group (−51.45 ± 15.75 mV) than in the control (−32.83 ± 7.57 mV) and wash (−43.14 ± 10.21 mV) groups (Fig. 2, E and F; Supplemental Fig. 1A).

LCA Dampens Excitability of DRG Neuron. Na_V channels play a key role in regulating action potentials in DRG neurons (Griffith et al., 2019; McDermott et al., 2019). We used the current clamp to record the changes of action potential before and after LCA treatment and to see whether the inhibition of Na_V channels by LCA could affect the DRG neuron excitability. We found that LCA significantly decreased the firing number (control group, 8.00 ± 5.55; LCA-treated group, 0.80 ± 1.16; wash group, 3.80 ± 1.60) and APP (control group, 104.68 ± 6.31 mV; LCA-treated group, 30.53 ± 20.35 mV; wash group, 93.66 ± 10.62 mV) of the DRG neurons (Fig. 3, A–C; Supplemental Fig. 1B). LCA did not significantly change the action potential threshold (control group, −42.75 ± 5.12 mV; LCA-treated group, −43.57 ± 5.77 mV; wash group, −43.21 ± 7.65 mV) or RP (control group, −59.44 ± 9.80 mV; LCA-treated group, −62.80 ± 10.33 mV; wash group, −63.64 ± 12.90 mV) of the DRG neurons (Fig. 3, D and E; Supplemental Fig. 1B). The results of the current clamp indicate that LCA could decrease the frequency and amplitude of the action potentials, thus dampening the excitabilities of DRG neurons.

The Effects of Licorice Extract on Na_V Current of DRG Neuron. It has been reported that LCA is a constituent exclusively produced by *G. inflata* Batalin in Xinjiang (Miyazaki et al., 2020). We used ethyl acetate to extract the flavonoids from the roots of *G. inflata* Batalin and detected LCA as the main constituents in this species with HPLC analysis (Fig. 4, A–C). It is of interest to see whether the effects of *G. inflata* Batalin extract are consistent with single-compound LCA. We applied the *G. inflata* Batalin extract on DRG neurons and recorded the Na_V currents. The content of LCA in *G. inflata* Batalin roots was 2.22% according to the peak area in HPLC chromatography. The concentration of LCA in *G. inflata* Batalin extract solution was 30 μμ for electrophysiological recordings on DRG neurons. The flavonoids extracted from another species, *G. uralensis* Fisch., which does not contain LCA, was used as negative control and applied with the same mass-to-volume ratio (0.046 mg/mL) (Fig. 4D). The *G. inflata* Batalin extract could significantly inhibit Na_V currents in DRG neurons, and the inhibition percentage was 77.06 ± 5.92%, whereas the *G. uralensis* Fisch. extract did not show significant inhibition on Na_V currents (Fig. 4, E and F). These results indicate that the effects of *G. inflata* Batalin extract on Na_V currents in DRG neuron were similar with single-compound LCA.

LCA Inhibits $Na_V1.7$ Channel Exogenously Expressed in HEK293T Cell. The Na_V channels expressed in DRG neurons could be divided into TTX-sensitive and TTX-resistant types

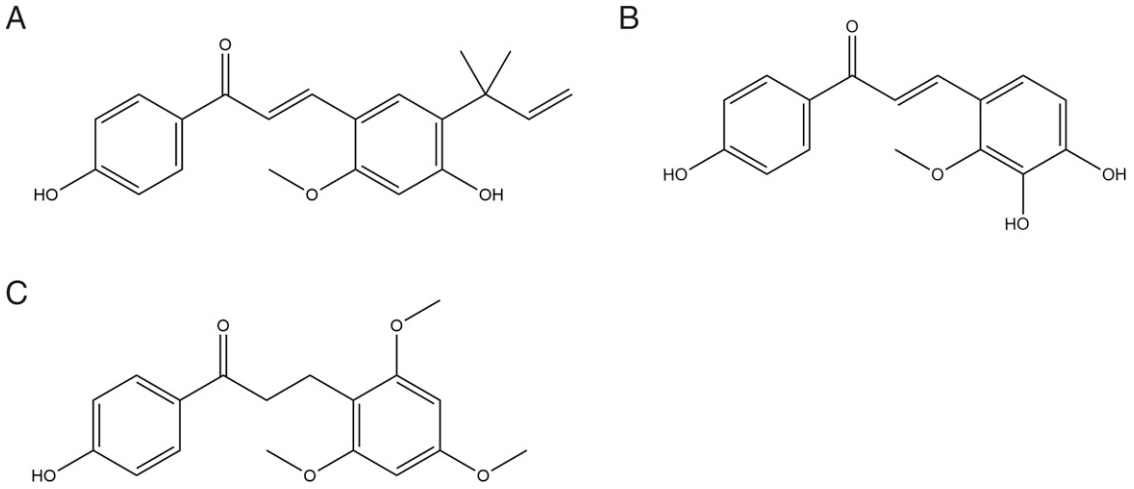

Fig. 1. Chemical structures of licochalcone A (A), licochalcone B (B), and loureirin B (C).

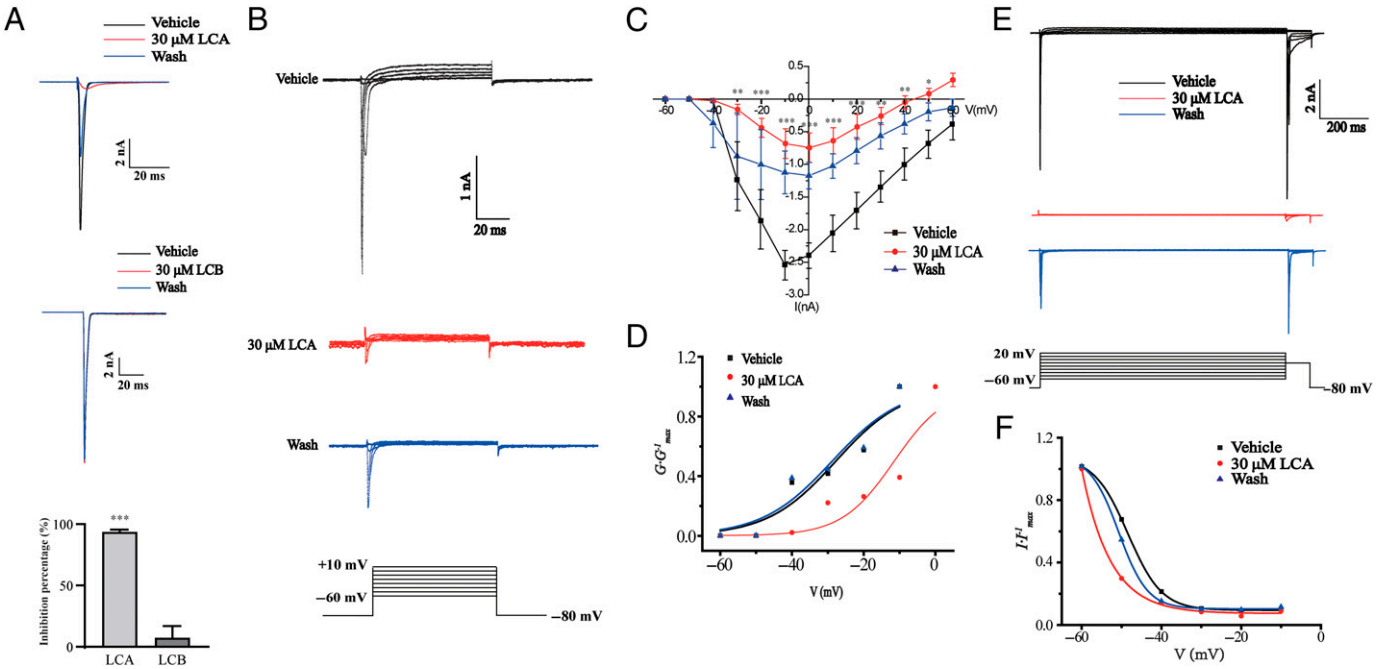

Fig. 2. Effects of LCA and LCB on Na_V currents in DRG neurons. (A) Representative traces of Na_V currents in DRG neurons under vehicle, 30 μM LCA (top) or LCB (middle), and wash treatments; statistics of the inhibition percentage of LCA (n = 7) and LCB (n = 5) compared with vehicle (bottom). (B) Representative traces of Na_V currents in DRG neurons with activation stimulus: cells were clamped at −80 mV, and Na_V currents were elicited from −60 mV to +10 mV in 10-mV steps for 100 milliseconds. (C) I-V curves of vehicle, LCA treatment, and wash groups. (D) Activation curves of vehicle, LCA, and wash treatments on single cell. (E) Representative traces of Na_V currents in DRG neurons with inactivation stimulus: Na_V currents were elicited from −60 mV to +10 mV in 10-mV steps for 1000 milliseconds, then kept at −20 mV for 100 milliseconds. (F) Inactivation curves of control, LCA, and wash treatments on single cell. All data are presented as mean ± S.E.M. for n independent observations. Statistical analysis of inhibition percentage was carried out using one-sample *t* test, and differences between groups was carried out using two-way ANOVA combined with Turkey post hoc test. $^*P < 0.05$; $^{**}P < 0.01$; $^{***}P < 0.001$.

(Ho and O'Leary, 2011; Li et al., 2018; Griffith et al., 2019). TTX-sensitive Na_V channels are expressed in both large- (>30 μm) and small-diameter (<30 μm) DRG neurons, whereas TTX-resistant Na_V channels are dominantly expressed in small-diameter DRG neurons (Ho and O'Leary, 2011; Li et al., 2018; Griffith et al., 2019). To identify which kind of Na_V currents were inhibited by LCA, 300 nM TTX diluted with external solution was applied after drug treatment in large-diameter DRG neurons. The Na_v currents were recovered to the same level before LCA treatment with external solution perfusion and TTX was applied to see whether the Na_v currents could be inhibited by the TTX. The Na_V currents which could be completely inhibit by 300 nM TTX was putative TTX-sensitive and analyzed (Fig. 5A). The statistics analysis of I-V curves showed that the maximum activation voltage and the half-activation voltage were significantly higher in the 30-μM LCA treatment group than in the control and wash groups (Fig. 5, B–D; Supplemental Fig. 1C). Then we tested the effects of LCA on TTX-resistant Na_V channels in small-diameter DRG neurons. Three hundred nanomolars of TTX was applied in the recording bath and drug perfusion solution. The residual Na_V currents were putative TTX-resistant

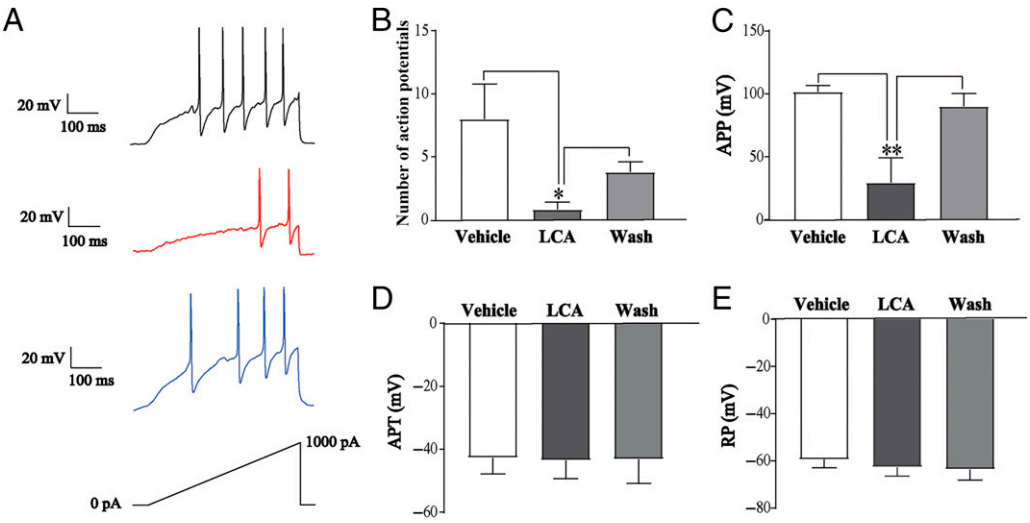

Fig. 3. Effects of LCA on action potentials of DRG neurons. (A) Representative action potential traces of DRG neurons under vehicle (black), LCA treatment (red), and wash (blue). Cells were clamped with rest membrane potentials and elicited with 0–1000 pA ramp current for 500 milliseconds. (B–E) Statistics of the number of action potentials (B), APP (C), action potential threshold (APT) (D), and RP (E) in DRG neurons with LCA treatment. All data are presented as mean ± S.E.M. for n independent observations. Statistical analysis of differences between groups was carried out using one-way ANOVA combined with Turkey post hoc test. $^*P < 0.05$; $^{**}P < 0.01$.

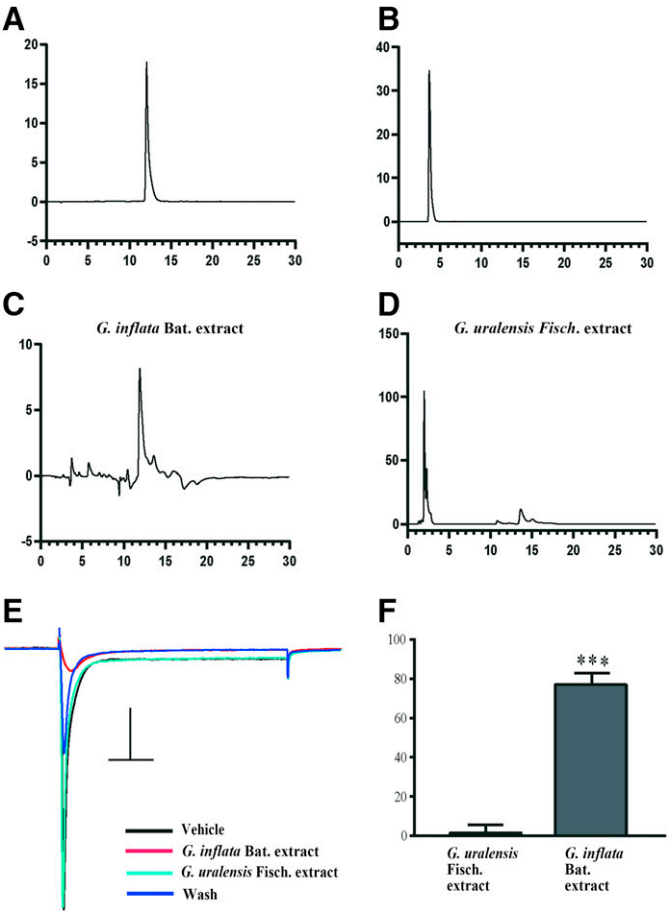

Fig. 4. Effects of licorice extract on Na_V channels of DRG neurons. (A) HPLC profiles of standard LCA samples; there is a single peak at 12.07 minutes. (A) HPLC profiles of standard LCB samples; there is a single peak at 3.72 minutes. (C) HPLC profiles of ethyl acetate *G. inflata* Batalin extract; the peak at 11.99 minutes is putative to be LCA, and the content of LCA in *G. inflata* Batalin is 2.22%. (D) HPLC profiles of *G. uralensis* Fisch. Flavonoids. (E) Representative traces of Na_V currents in DRG neurons under vehicle (black), *G. inflata* Batalin extract (red), *G. uralensis* Fisch. flavonoids (cyan), and wash (blue) treatments; the mass:volume ratio of *G. inflata* Batalin extract used was 0.046 mg/mL to guarantee a 30-μM concentration of LCA. (F) Inhibition percentage of *G. uralensis* Fisch. and *G. inflata* Batalin extract on Na_V currents of DRG neurons (n = 4); the data are presented as mean ± S.E.M. Statistical analysis of differences between the two groups was carried out using Student's *t* test. ***$P < 0.001$.

currents (Fig. 5E). The statistical analysis of I-V curves showed that the maximum activation voltage and the half-activation voltage were higher in the 30-μM LCA treatment group than in the control and wash groups (Fig. 5, F–H; Supplemental Fig. 1D). These results indicate that LCA could exert inhibition effects on both TTX-sensitive and TTX-resistant Na_V channels.

According to the above results, the large-diameter DRG neurons exclusively expressing TTX-sensitive channels could be blocked by LCA. We expressed one subunit of TTX-sensitive Na_V channel—$Na_V1.7$—in HEK293T cells to observe the effects of LCA. Our results showed that LCA could both inhibit $Na_V1.7$ currents and shift the I-V curve to depolarization direction (Fig. 6, A–C). Analysis on voltage-gating properties indicated that LCA did not significantly increase the half-activation voltage of $Na_V1.7$ channel (Fig. 6D; Supplemental Fig. 1E), whereas LCA significantly decreased the fast and slow half-inactivation voltage of $Na_V1.7$ channel (Fig. 6, E and F; Supplemental Fig. 1E). To get the IC_{50} value of LCA on $Na_V1.7$, we treated the $Na_V1.7$-expressing HEK293T cells with different concentrations of LCA for 1.5 minutes. The IC_{50} value (7.6 ± 3.5 μM; $n = 5$) was calculated by fitting concentration-response curve to Hill equation (Fig. 6G). We also applied LCB on HEK293T cells expressing $Na_V1.7$ and analyzed the voltage-gating properties. The half-activation and inactivation voltage of $Na_V1.7$ channel were not significantly changed by LCB (Fig. 7, A–E).

The Effects of LCA and LCB on Formalin-Induced Pain Responses. $Na_V1.7$ has been reported to be predominantly expressed in nociceptors and closely related to pain in humans and animals (Kingwell, 2019; McDermott et al., 2019). Since LCA had significant inhibition effects on Na_V currents in DRG neurons and $Na_V1.7$ channels exogenously expressed in HEK293T cells, it might also have pain-relief effects. We used a pain behavior model - formalin test to investigate the effects of LCA on acute pain responses of animals (Uniyal et al., 2021). There are two phases in formalin tests: the first phase was mainly conducted by neuropathic pain, whereas the second phase was related to the activation of complex downstream pathways (Fernandes et al., 2018; Uniyal et al., 2021). Our results showed that different concentrations (25 mg/kg, 50 mg/kg, and 100 mg/kg) of LCA could alleviate the pain responses in both the first and the second phases of the formalin test (Fig. 8, A and B). We applied 50 mg/kg mexiletine, which is a known Na_V channel blocker and analgesic drug, as the positive control during the tests (Blackburn-Munro et al., 2002). The results of mexiletine showed that it could significantly decrease the licking time of mice after formalin injection in their right hind paws during both phases, which confirmed that our animal models are successful. The effects of LCA were consistent with their effects on Na_V channels in DRG neurons and $Na_V1.7$ expressed in HEK293T cells. LCB did not affect the responses during the first phase of formalin test but could inhibit the licking time during the second phase in a relatively high concentration (100 mg/kg) (Fig. 8, C and D). These results indicate that LCB behaves differently with LCA on Na_V channels and neuropathic pain but may exert effects on molecular signaling pathways during the second phase of formalin test.

Discussion

As a traditional Chinese medicine, licorice is commonly applied to protect the stomach and spleen, alleviate pain, and improve the symptoms of cough and phlegm (Yang et al., 2015). Researchers recently discovered that LCA could relieve neuropathic pain and inflammatory responses (Chu et al., 2012; Li et al., 2021). Although licorice was proved to have effects on multiple diseases, the molecular mechanisms have rarely been disclosed. LCA and LCB are chalcones in licorice and share the same backbones with each other. The results of electrophysiological recording showed that LCA could inhibit Na_V currents in DRG neurons. These results indicate that LCA has the potential to be developed into Na_V inhibitors. Although LCA could significantly inhibit Na_V currents in mouse DRG cells, LCB did not block the Na_V currents. LCB also did not have effects on activation or inactivation of $Na_V1.7$ channel. Structural analysis showed that the predicted physicochemical properties of LCA and LCB, such as LogP and pKa,

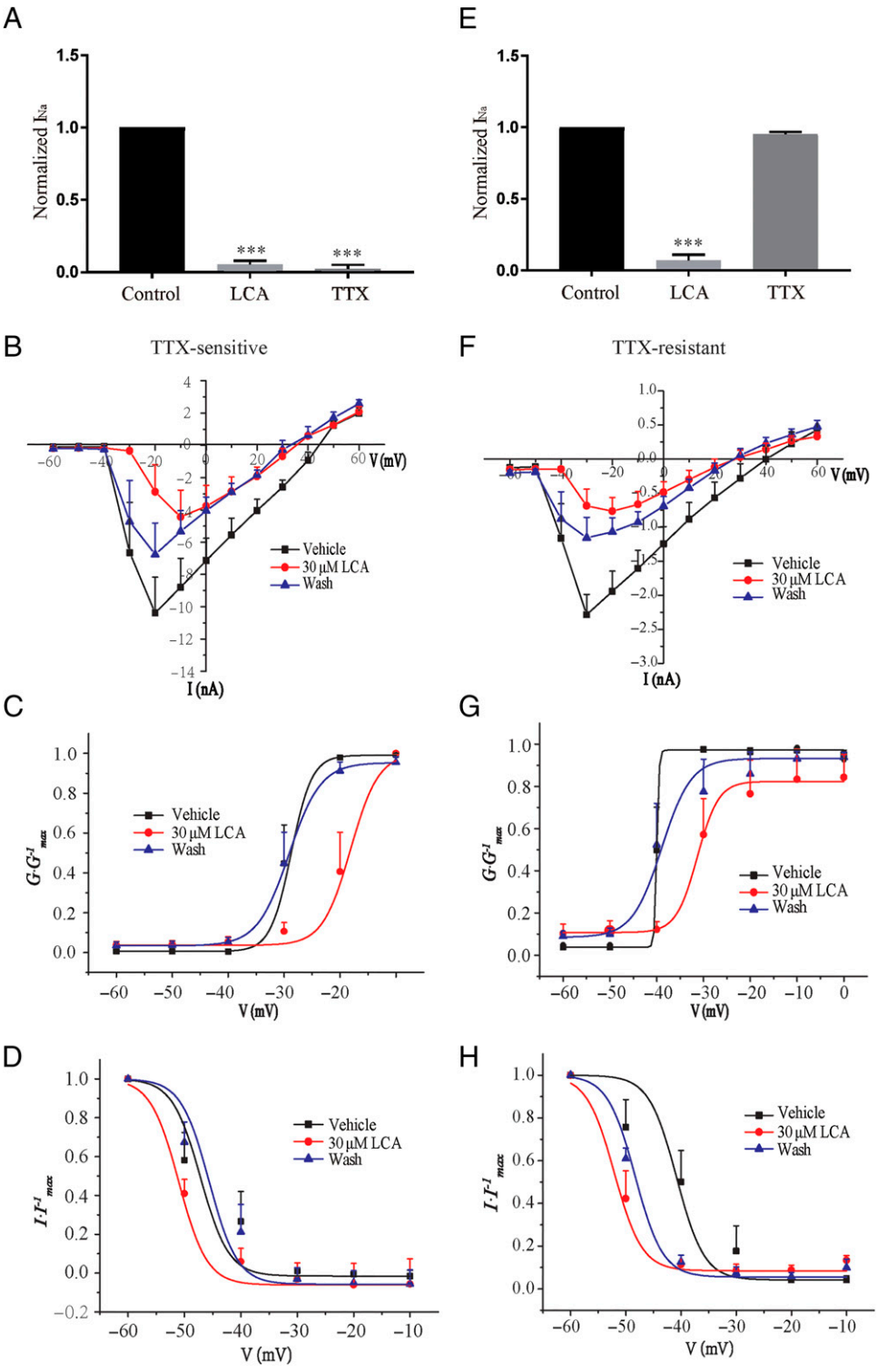

Fig. 5. Effects of LCA on TTX-sensitive and TTX-resistant Na_V channels. (A) Statistics of TTX-sensitive Na_V currents recorded from large-diameter DRG neurons. (B–D) I-V curve (B), activation curve (C), and inactivation curve (D) of TTX-sensitive Na_V currents under vehicle, 30 μM LCA, and wash treatments. (E) Statistics of TTX-resistant Na_V currents recorded from small-diameter DRG neurons. (F–H) I-V curve (F), activation curve (G), and inactivation curve (H) of TTX-resistant Na_V currents under vehicle, 30 μM LCA, and wash treatments. All data are presented as mean ± S.E.M. for n independent observations. Statistical analysis of differences between groups was carried out using one-way ANOVA combined with Turkey post hoc test. ***$P < 0.001$.

are different (data not shown). This might be because LCA has olefin substituents consisting of five carbon atoms on the aromatic B ring, whereas LCB has no such side chain but one extra hydroxyl group, which suggests that the olefin substituent on the aromatic B ring of licochalcone may play a key role in blocking the Na_V channel. The discrepancy of effects between LCA and LCB may guide us to discover the key chemical groups to inhibit the specific channels and develop more effective Na_V channel inhibitors.

Na_V channels in DRG neurons could modulate the membrane potential oscillations and transduce sensories, like pain and itch (Li et al., 2018; Griffith et al., 2019). We used current clamp to record the action potentials of DRG neurons to see whether inhibition of Na_V channels by LCA could dampen the excitabilities of these neurons. The results showed that LCA could significantly decrease the firing frequencies and amplitudes of DRG neurons. We further conducted formalin test

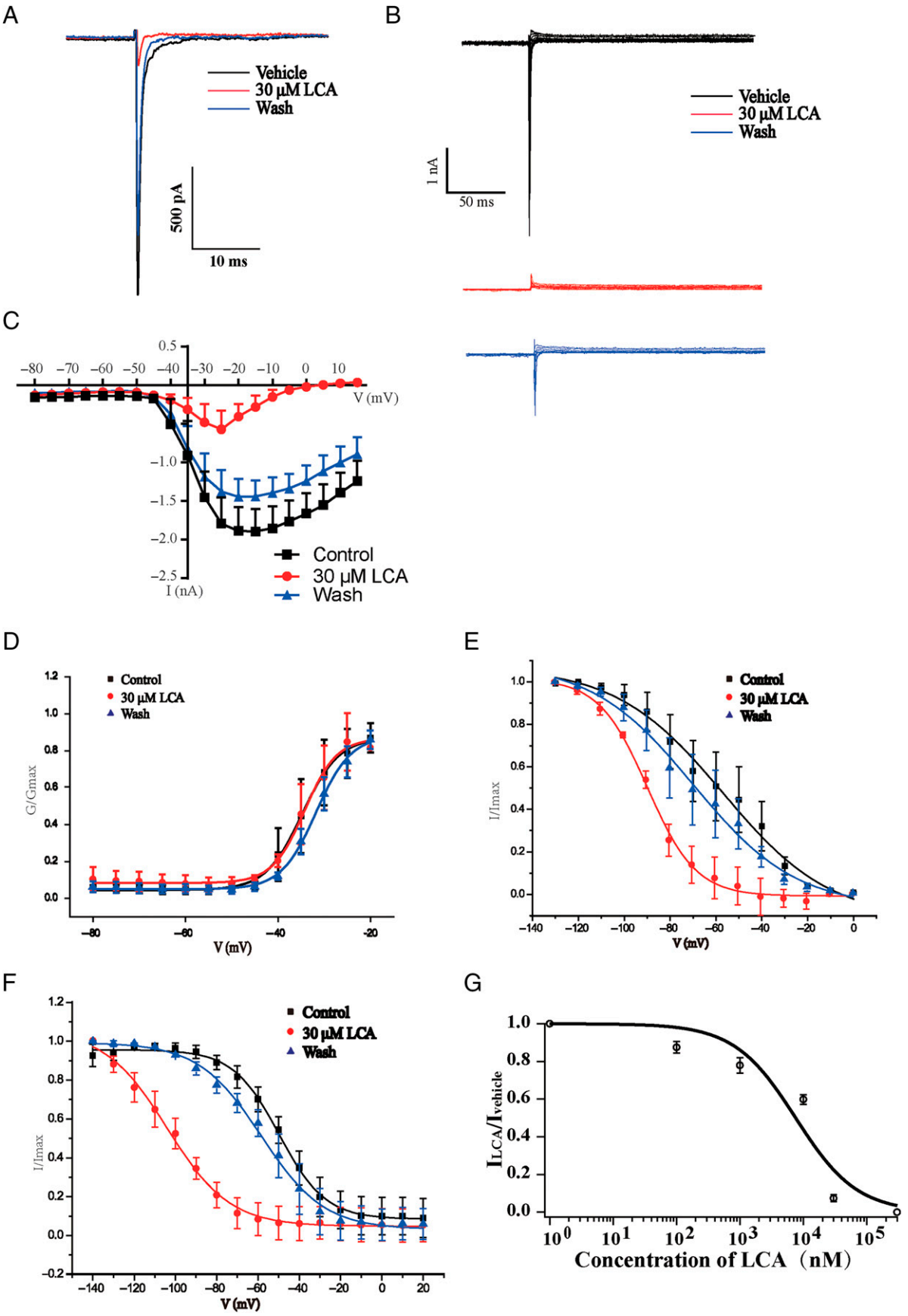

Fig. 6. Effects of LCA on $Na_V1.7$ channels exogenously expressed on HEK293T cells. (A) Representative traces of $Na_V1.7$ currents in HEK293T cells before or after LCA treatment. (B) Representative traces of Na_V currents in DRG neurons with activation stimulus: cells were clamped at −120 mV, and Na_V currents were elicited from −80 mV to 15 mV in 5-mV steps for 50 milliseconds. (C) I-V curves of $Na_V1.7$ channel *(Continued)*

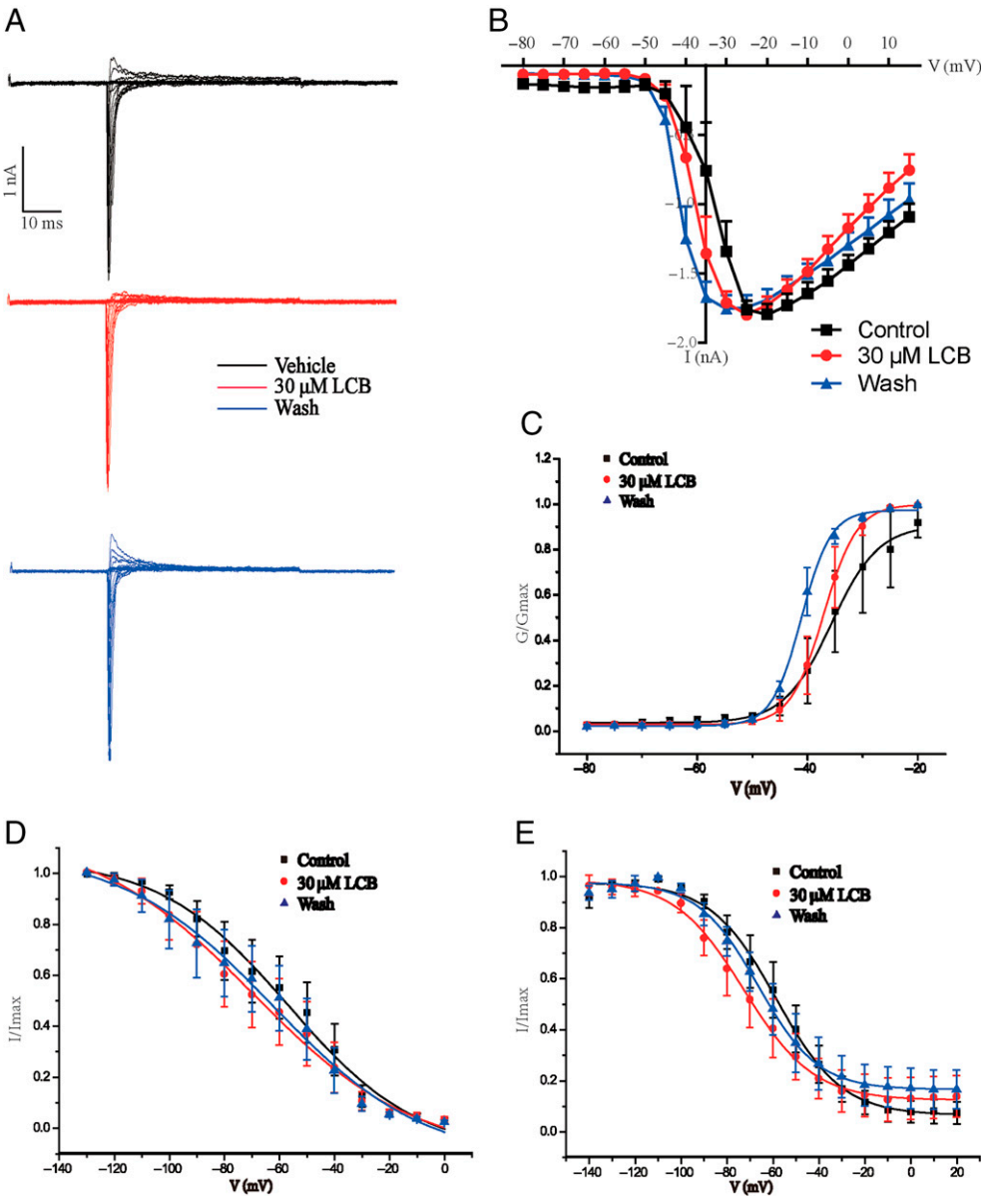

Fig. 7. Effects of LCB on $Na_V1.7$ channels exogenously expressed on HEK293T cells. (A) Representative traces of Na_V currents in HEK293T cells with activation stimulus: cells were clamped at −120 mV, and Na_V currents were elicited from −80 mV to 15 mV in 5-mV steps for 50 milliseconds. (B) I-V curves of $Na_V1.7$ channel with LCA treatment; the data are presented as mean ± S.E.M. for n independent observations, and statistical analysis of differences between groups was carried out using two-way ANOVA combined with Turkey post hoc test. (C–E) Activation curves (C), fast inactivation curves (D), and slow inactivation curves (E) with LCB treatment.

and observed that LCA had analgesic effects in these animal models. It has been confirmed that pain responses during phase 1 of formalin test is neuropathic pain, which is mediated by direct nociceptor neurotransmission, whereas phase2 involves more complex signaling pathways, such as immune cell infiltration and the activation of glia (Fernandes et al., 2018; Uniyal et al., 2021). Our results showed that LCA could decrease the licking time of mice during both phase 1 and phase 2 of formalin test. These results were consistent with changes of Na_V currents in DRG neurons and inhibition of $Na_V1.7$ exogenously expressed in HEK293T cells. Previous studies have reported that $Na_V1.7$ is widely expressed in DRG neurons and is devoted both to neuropathic pain and inflammatory pain (Nassar et al., 2004; Dib-Hajj et al., 2013). Inhibition of $Na_V1.7$ by LCA may lead to alleviation of pain responses during both phase 1 and phase 2 in formalin test. Although LCB did not show inhibitory effects on DRG Na_V currents, it could decrease the licking time during phase 2 of formalin test. We suspect that LCB may be able to inhibit other channels or signaling molecules that were involved in the pain or inflammatory responses during phase 2. It is of great interest to explore the mechanisms of this phenomenon.

DRG neurons could be divided into diverse groups according to their size, function, and molecular characteristics (Ho and

with LCA treatment; the data are presented as mean ± S.E.M. for n independent observations, and statistical analysis of differences between groups was carried out using two-way ANOVA combined with Turkey post hoc test. (D–F) Activation curves (D), fast inactivation curves (E), and slow inactivation curves (F) with LCA treatment. (G) Concentration- response curve of $Na_V1.7$ current with LCA treatment; y-axis represents the ratios of Na_V current amplitudes ($I_{LCA}/I_{vehicle}$), and x-axis represents the concentration of LCA. The curve was fitted by Hill equation.

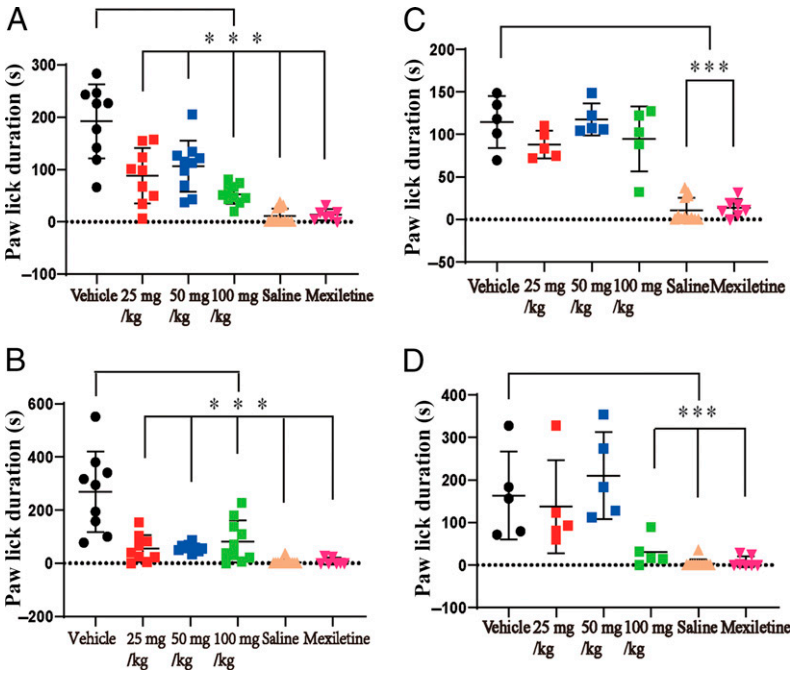

Fig. 8. Effects of LCA and LCB on formalin-induced pain responses. (A) Statistics of paw-licking time during the first phase of formalin test under vehicle (n = 9), LCA in different concentrations (n = 9 for 25 mg/kg, n = 10 for 50 mg/kg, and n = 10 for 100 mg/kg), saline (n = 12), and Mexiletine (n = 7) treatments. (B) Statistics of paw-licking time during the second phase of formalin test under vehicle, LCA in different concentrations, saline, and mexiletine treatments. (C) Statistics of paw-licking time during the first phase of formalin test under vehicle (n = 5), LCB in different concentrations (n = 5 for 25 mg/kg, n = 5 for 50 mg/kg, and n = 5 for 100 mg/kg), saline (n = 12), and mexiletine (n = 7) treatments. (D) Statistics of paw-licking time during the second phase of formalin test under vehicle, LCA in different concentrations, saline, and mexiletine treatments. All data are presented as mean ± S.E.M. for n independent observations. Statistical analysis of differences between groups was carried out using two-way ANOVA combined with Turkey post hoc test. *$P < 0.05$; **$P < 0.01$; ***$P < 0.001$ compared with the vehicle group.

O'Leary, 2011; Dib-Hajj et al., 2013). Small-size (<30 μm) DRG neurons express both TTX-sensitive Na_V channels, such as $Na_V1.7$, and TTX-resistant Na_V channels, such as $Na_V1.8$ and $Na_V1.9$ (Ho and O'Leary, 2011; Griffith et al., 2019). Large-size (>30 μm) DRG neurons mainly express TTX-sensitive Na_V channels, such as $Na_V1.1$, $Na_V1.6$, and $Na_V1.7$ (Ho and O'Leary, 2011; Griffith et al., 2019). Three hundred nanomolars of TTX was applied after LCA administration and wash-back in large-size DRG neurons to confirm that the recorded Na_V currents could be completely blocked. The results indicated that LCA could inhibit TTX-sensitive Na_V channels in large-size DRG neurons. Although we observed the inhibition on Nav1.7 in HEK293T cells, the effects of LCA on other subunits, such as Nav1.1 and Nav1.6, need to be explored. To separate the TTX-resistant Na_V currents, 300 nM TTX was applied in the bath solution ,and the residual Na_V currents in small-size DRG neurons were recorded. Similar to the results in large-size DRG neurons, LCA could inhibit TTX-resistant Na_V currents in these cells. These results indicate that LCA may be able to inhibit TTX-resistant Na_V channels, like $Na_V1.8$ and $Na_V1.9$. We need further express other types of Na_V channel subunits in HEK293T cells to observe the effects of LCA in future.

Authorship Contributions

Participated in research design: Yin.

Conducted experiments: Zhao, Zhang, Long, Wang, Yu, Zhou, Li, Xue, Hu.

Performed data analysis: Zhao, Zhang, Long, Wang, Yin.

Wrote or contributed to the writing of the manuscript: Zhao, Yin.

References

Adianti M, Aoki C, Komoto M, Deng L, Shoji I, Wahyuni TS, Lusida MI, Soetjipto, Fuchino H, Kawahara N, et al. (2014) Anti-hepatitis C virus compounds obtained from Glycyrrhiza uralensis and other Glycyrrhiza species. *Microbiol Immunol* **58**:180–187.

Ahn SJ, Cho EJ, Kim HJ, Park SN, Lim YK, and Kook JK (2012) The antimicrobial effects of deglycyrrhizinated licorice root extract on Streptococcus mutans UA159 in both planktonic and biofilm cultures. *Anaerobe* **18**:590–596.

Blackburn-Munro G, Ibsen N, and Erichsen HK (2002) A comparison of the anti-nociceptive effects of voltage-activated Na+ channel blockers in the formalin test. *Eur J Pharmacol* **445**:231–238.

Chang W, Berta T, Kim YH, Lee S, Lee SY, and Ji RR (2018) Expression and Role of Voltage-Gated Sodium Channels in Human Dorsal Root Ganglion Neurons with Special Focus on Nav1.7, Species Differences, and Regulation by Paclitaxel. *Neurosci Bull* **34**:4–12.

Chen S, Wan Y, Liu X, and Pan X (2018) Inhibitive effect of loureirin B plus capsaicin on tetrodotoxin-resistant sodium channel. *J Tradit Chin Med* **38**:842–852.

Chu X, Ci X, Wei M, Yang X, Cao Q, Guan M, Li H, Deng Y, Feng H, and Deng X (2012) Licochalcone a inhibits lipopolysaccharide-induced inflammatory response in vitro and in vivo. *J Agric Food Chem* **60**:3947–3954.

Dib-Hajj SD and Waxman SG (2019) Sodium Channels in Human Pain Disorders: Genetics and Pharmacogenomics. *Annu Rev Neurosci* **42**:87–106.

Dib-Hajj SD, Yang Y, Black JA, and Waxman SG (2013) The Na(V)1.7 sodium channel: from molecule to man. *Nat Rev Neurosci* **14**:49–62.

Dustrude ET, Moutal A, Yang X, Wang Y, Khanna M, and Khanna R (2016) Hierarchical CRMP2 posttranslational modifications control NaV1.7 function. *Proc Natl Acad Sci USA* **113**:E8443–E8452.

Fernandes V, Sharma D, Vaidya S, P A S, Guan Y, Kalia K, and Tiwari V (2018) Cellular and molecular mechanisms driving neuropathic pain: recent advancements and challenges. *Expert Opin Ther Targets* **22**:131–142.

Fertleman CR, Baker MD, Parker KA, Moffatt S, Elmslie FV, Abrahamsen B, Ostman J, Klugbauer N, Wood JN, Gardiner RM, et al. (2006) SCN9A mutations in paroxysmal extreme pain disorder: allelic variants underlie distinct channel defects and phenotypes. *Neuron* **52**:767–774.

Gingras J, Smith S, Matson DJ, Johnson D, Nye K, Couture L, Feric E, Yin R, Moyer BD, Peterson ML, et al. (2014) Global Nav1.7 knockout mice recapitulate the phenotype of human congenital indifference to pain. *PLoS One* **9**:e105895.

Goldfarb M, Schoorlemmer J, Williams A, Diwakar S, Wang Q, Huang X, Giza J, Tchetchik D, Kelley K, Vega A, et al. (2007) Fibroblast growth factor homologous factors control neuronal excitability through modulation of voltage-gated sodium channels. *Neuron* **55**:449–463.

Griffith TN, Docter TA, and Lumpkin EA (2019) Tetrodotoxin-Sensitive Sodium Channels Mediate Action Potential Firing and Excitability in Menthol-Sensitive Vglut3-Lineage Sensory Neurons. *J Neurosci* **39**:7086–7101.

Ho C and O'Leary ME (2011) Single-cell analysis of sodium channel expression in dorsal root ganglion neurons. *Mol Cell Neurosci* **46**:159–166.

Hong SH, Cha HJ, Hwang-Bo H, Kim MY, Kim SY, Ji SY, Cheong J, Park C, Lee H, Kim GY, et al. (2019) Anti-Proliferative and Pro-Apoptotic Effects of Licochalcone A through ROS-Mediated Cell Cycle Arrest and Apoptosis in Human Bladder Cancer Cells. *Int J Mol Sci* **20**:3820.

Kingwell K (2019) Nav1.7 withholds its pain potential. *Nat Rev Drug Discov DOI:* 10.1038/d41573-019-00065-0 [published ahead of print].

Li P, Yu C, Zeng FS, Fu X, Yuan XJ, Wang Q, Fan C, Sun BL, and Sun QS (2021) Licochalcone A Attenuates Chronic Neuropathic Pain in Rats by Inhibiting Microglia Activation and Inflammation. *Neurochem Res* **46**:1112–1118.

Li Y, North RY, Rhines LD, Tatsui CE, Rao G, Edwards DD, Cassidy RM, Harrison DS, Johansson CA, Zhang H, et al. (2018) DRG Voltage-Gated Sodium Channel 1.7 Is Upregulated in Paclitaxel-Induced Neuropathy in Rats and in Humans with Neuropathic Pain. *J Neurosci* **38**:1124–1136.

Liu Q, Bhat M, Bowen WD, and Cheng J (2009) Signaling pathways from cannabinoid receptor-1 activation to inhibition of N-methyl-D-aspartic acid mediated calcium

influx and neurotoxicity in dorsal root ganglion neurons. *J Pharmacol Exp Ther* **331**:1062–1070.
McDermott LA, Weir GA, Themistocleous AC, Segerdahl AR, Blesneac I, Baskozos G, Clark AJ, Millar V, Peck LJ, Ebner D, et al. (2019) Defining the Functional Role of $Na_V1.7$ in Human Nociception. *Neuron* **101**:905–919.e8.
McNamara CR, Mandel-Brehm J, Bautista DM, Siemens J, Deranian KL, Zhao M, Hayward NJ, Chong JA, Julius D, Moran MM, et al. (2007) TRPA1 mediates formalin-induced pain. *Proc Natl Acad Sci USA* **104**:13525–13530.
Miyazaki A, Eerdunbayaer, Shiokawa T, Tada H, Lian Y, Taniguchi S, and Hatano T (2020) High-performance liquid chromatographic profile and ^1H quantitative nuclear magnetic resonance analyses for quality control of a Xinjiang licorice extract. *Biosci Biotechnol Biochem* **84**:2128–2138.
Nassar MA, Stirling LC, Forlani G, Baker MD, Matthews EA, Dickenson AH, and Wood JN (2004) Nociceptor-specific gene deletion reveals a major role for Nav1.7 (PN1) in acute and inflammatory pain. *Proc Natl Acad Sci USA* **101**:12706–12711.
Shi S, Zhao Q, Ke C, Long S, Zhang F, Zhang X, Li Y, Liu X, Hu H, and Yin S (2021) Loureirin B Exerts its Immunosuppressive Effects by Inhibiting STIM1/Orai1 and $K_V1.3$ Channels. *Front Pharmacol* **12**:685092.
The Committee of Pharmacopoeia of the People's Republic of China (1995) *Pharmacopoeia of the People's Republic of China*, 1st ed, Science and technology publisher of Guangdong, Guangzhou, Chemical and industry Press, Beijing.
Uniyal A, Shantanu PA, Vaidya S, Belinskaia DA, Shestakova NN, Kumar R, Singh S, and Tiwari V (2021) Tozasertib Attenuates Neuropathic Pain by Interfering with Aurora Kinase and KIF11 Mediated Nociception. *ACS Chem Neurosci* **12**:1948–1960.
Wu MT, Huang PY, Yen CT, Chen CC, and Lee MJ (2013) A novel SCN9A mutation responsible for primary erythromelalgia and is resistant to the treatment of sodium channel blockers. *PLoS One* **8**:e55212.
Xu B, Mo C, Lv C, Liu S, Li J, Chen J, Wei Y, An H, Ma L, and Guan X (2019) Post-surgical inhibition of phosphatidylinositol 3-kinase attenuates the plantar incision-induced postoperative pain behavior via spinal Akt activation in male mice. *BMC Neurosci* **20**:36.
Yang R, Wang LQ, Yuan BC, and Liu Y (2015) The Pharmacological Activities of Licorice. *Planta Med* **81**:1654–1669.
Yang Y, Wang Y, Li S, Xu Z, Li H, Ma L, Fan J, Bu D, Liu B, Fan Z, et al. (2004) Mutations in SCN9A, encoding a sodium channel alpha subunit, in patients with primary erythermalgia. *J Med Genet* **41**:171–174.
Yuan J, Matsuura E, Higuchi Y, Hashiguchi A, Nakamura T, Nozuma S, Sakiyama Y, Yoshimura A, Izumo S, and Takashima H (2013) Hereditary sensory and autonomic neuropathy type IID caused by an SCN9A mutation. *Neurology* **80**:1641–1649.
Zheng YM, Wang WF, Li YF, Yu Y, and Gao ZB (2018) Enhancing inactivation rather than reducing activation of Nav1.7 channels by a clinically effective analgesic CNV1014802. *Acta Pharmacol Sin* **39**:587–596.
Zhong XL, Wei R, Zhou P, Luo YW, Wang XQ, Duan J, Bi FF, Zhang JY, Li CQ, Dai RP, et al. (2012) Activation of Anterior Cingulate Cortex Extracellular Signal-Regulated Kinase-1 and -2 (ERK1/2) Regulates Acetic Acid-Induced, Pain-Related Anxiety in Adult Female Mice. *Acta Histochem Cytochem* **45**:219–225.

Address correspondence to: Shijin Yin, Department of Chemical Biology, School of Pharmaceutical Sciences, South-Central Minzu University, No.182 Minzu Road, Hongshan District, Wuhan, Hubei Province, 430074, People's Republic of China. E-mail: yinshijinyf@163.com